Ultrafast Inorganic Scintillators for Gigahertz Hard X-Ray Imaging

Chen Hu, *Member, IEEE*, Liyuan Zhang, *Member, IEEE*, Ren-Yuan Zhu, *Senior Member, IEEE*, Aiping Chen, Zhehui Wang, *Member, IEEE*, Lei Ying, and Zongfu Yu

***Abstract*— Gigahertz hard X-ray imaging for the proposed matter-radiation interaction in extreme project presents an unprecedented challenge to front imager in both speed and radiation hardness. Novel fast scintillators are to be developed to face these challenges. This paper presents an investigation on the optical and scintillation properties for a set of fast inorganic scintillators. Transmittance, emission, light output, and decay time were measured. Based on this investigation, we plan to take two approaches to develop inorganic scintillators with subnanoseconds of decay time for the gigahertz hard X-ray imaging. One is yttrium-doped barium fluoride single crystals, and another is based on gallium-doped ZnO nanoparticles.**

***Index Terms*— Hard X-ray imaging, light output (LO), self-absorption, transmittance, ultrafast decay time, ultrafast scintillator.**

I. Introduction

AIMING at studying the dynamics of material evolution related to the nuclear Big Bang, the matter–radiation interaction in extreme (MaRIE) experimental facility was proposed at Los Alamos [1], [2], where gigahertz hard X-ray (>20 keV) imaging is required. The proposed X-ray energy and the interframe time are 30 keV and 2 ns in phase I and up to 126 keV and 300 ps in phase II, respectively [3]. These ultrafast interframe times require ultrafast sensors to capture and store the dense spatial and temporal signals. To mitigate pileup effect for such high frame rates, it is important to have a temporal response of less than 2 ns and 300 ps, respectively, for the Type I and II imagers. The development of sensors with ultrafast time response is thus important as well [3].

Fig. 1 is a schematic showing an inorganic scintillator-based total absorption imager concept featured with a pixelated ultrafast scintillator screen, a pixelated ultrafast photodetector, and ultrafast readout electronics [3].

Table I summarizes the basic properties of various fast scintillators investigated in the recent years for gigahertz hard X-ray imaging with a reference of cerium-doped lutetium yttrium oxyorthosilicate LYSO:Ce crystal ($Lu_{2(1-x)}Y_{2x}SiO_5$:Ce or LYSO) and yttrium oxyorthosilicate (Y_2SiO_5:Ce or YSO:Ce), which are chosen because of their excellent performance and wide applications.

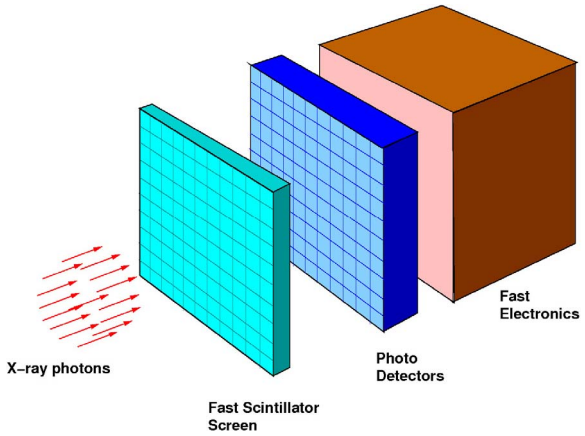

Fig. 1. Schematic showing total absorption concept of a pixelated crystal-based front imager for the proposed gigahertz X-ray imaging.

The crystal candidates listed in Table I can be classified into four groups according to their scintillation mechanism. The first group is the direct-gap semiconductor crystals, such as gallium-doped ZnO (ZnO:Ga). The second group is the core-valence luminescence crystals, such as BaF_2. The third group is Yb^{3+} activated crystals featured with fast decay time and thermal quenching, such as $YAlO_3$:Yb (YAP:Yb) and $Y_3Al_5O_{12}$:Yb (YAG:Yb). The fourth group is Ce^{3+}-activated bright and fast crystals, such as $YAlO_3$ (YAP:Ce), $Lu_3Al_5O_{12}$:Ce (LuAG:Ce), and $LaBr_3$:Ce.

The bright and fast halides, such as $LaBr_3$:Ce and $CeBr_3$, are highly hygroscopic, so that their application needs extra engineering work. Among the nonhygroscopic inorganic crystal scintillators listed in Table I, BaF_2 crystals with subnanoseconds of fast decay time provide high scintillation photon yield in the first nanoseconds. This fast scintillation component promises a solution for an ultrafast front imager. BaF_2 is also featured with the shortest attenuation length for 40-keV X-rays, promising a compact sensor for gigahertz hard X-ray imaging. Recent investigation on ZnO:Ga nanoparticles imbedded in polystyrene shows its ultrafast scintillation light with subnanoseconds decay time (0.5 ns) [5], which promises another solution for an ultrafast front imager for gigahertz hard X-ray imaging.

Manuscript received January 14, 2018; accepted February 15, 2018. Date of publication February 19, 2018; date of current version August 15, 2018. This work was supported by the U.S. Department of Energy, Office of High Energy Physics Program, under Award DE-SC0011925.

C. Hu, L. Zhang, and R.-Y. Zhu are with the Physics Department, California Institute of Technology, Pasadena, CA 91125 USA (e-mail: zhu@hep.caltech.edu).

A. Chen and Z. Wang are with the Los Alamos National Laboratory, Los Alamos, NM 87545 USA.

L. Ying and Z. Yu are with the Materials Science and Engineering Department, University of Wisconsin, Madison, WI 53706 USA.

Color versions of one or more of the figures in this paper are available online at http://ieeexplore.ieee.org.

Digital Object Identifier 10.1109/TNS.2018.2808103

TABLE I
CANDIDATE SCINTILLATORS FOR GIGAHERTZ HARD X-RAY IMAGING

	LYSO:Ce	YSO:Ce	ZnO:Ga	BaF_2	BaF_2:Y	YAP:Yb	YAG:Yb	YAP:Ce	LuAG:Ce	$LaBr_3$:Ce
Density (g/cm^3)	7.4	4.44	5.67	4.89	4.89	5.35	4.56	5.35	6.76	5.29
Melting Points (^oC)	2050	2070	1975	1280	1280	1870	1940	1870	2060	783
X_0 (cm)	1.14	3.10	2.51	2.03	2.03	2.77	3.53	2.77	1.45	1.88
R_M (cm)	2.07	2.93	2.28	3.1	3.1	2.4	2.76	2.4	2.15	2.85
λ_I (cm)	20.9	27.8	22.2	30.7	30.7	22.4	25.2	22.4	20.6	30.4
Z_{eff}	64.8	33.3	27.7	51.6	51.6	31.9	30	31.9	60.3	45.6
dE/dX (MeV/cm)	9.55	6.57	8.42	6.52	6.52	8.05	7.01	8.05	9.22	6.90
λ_{peak} [a] (nm)	420	420	380	300 220	300 220	350	350	370	520	360
Refractive Index[b]	1.82	1.78	2.1	1.50	1.50	1.96	1.87	1.96	1.84	1.9
Normalized Light Yield[a,c]	100	80	6.6[e]	42 4.8	1.7 4.8	0.19[e]	0.36[e]	9 32	35[f] 48[f]	153
Total Light Yield (ph/MeV)	30,000	24,000	2,000[e]	13,000	2,000	57[e]	110[e]	12,000	25,000[f]	46,000
Decay Time[a] (ns)	40	75	<1	600 0.6	600 0.6	1.5	4	191 25	820 50	20
Light Yield in 1st ns (photons/MeV)	740	318	610[e]	1200	1200	28[e]	24[e]	391	240	2,200
40 keV Att. Length (1/e, mm)	0.185	0.334	0.407	0.106	0.106	0.314	0.439	0.314	0.251	0.131

[a]Top line: slow component, bottom line: fast component.
[b]At the wavelength of the emission maximum.
[c]Excited by Gamma rays.
[d]For 0.4 at% Ca co-doping.
[e]Excited by Alpha particles.
[f]Ceramic with 0.3 Mg at% co-doping. [4]

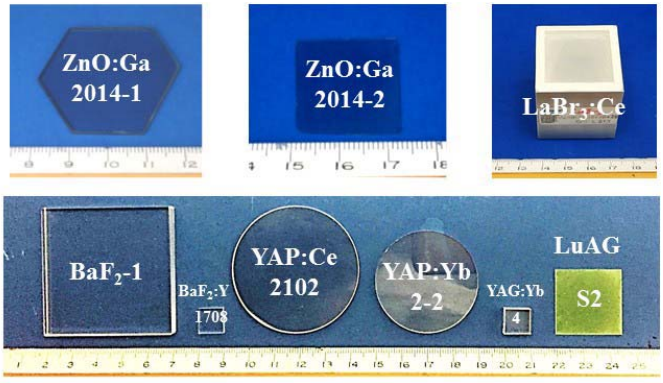

Fig. 2. Photograph showing samples investigated in this paper.

TABLE II
BASIC PROPERTIES FOR THE SAMPLES INVESTIGATED IN THIS PAPER

Crystal	Vendor	ID	Dimension (mm^3)
ZnO:Ga	FJIRSM	2014-1	33×30×2
ZnO:Ga	FJIRSM	2014-2	22×22×0.3
BaF_2	SIC	1	50×50×5
BaF_2:Y	BGRI	1708	10×10×5
YAP:Yb	DJ	2-2	Φ40×2
YAG:Yb	DJ	4	10×10×5
YAP:Ce	DJ	2102	Φ50×2
LuAG:Ce Ceramic	SIC	S2	25×25×0.4
$LaBr_3$:Ce	S-G	2	28×28×28

In this paper, we report the results on fast inorganic scintillators investigated at the Caltech HEP Crystal Laboratory. Their optical and scintillation properties, such as transmittance, emission, light output (LO), and decay time, are measured. The pros and cons of each of the four groups are discussed. For gigahertz hard X-ray imaging, yttrium-doped BaF_2 crystals (BaF_2:Y) and ZnO:Ga nanoparticle-based scintillators are most promising.

II. SAMPLES AND EXPERIMENTAL DETAILS

Fig. 2 shows photograph of inorganic crystal scintillator samples investigated. Their corresponding dimension information is listed in Table II. Two ZnO:Ga samples were produced in the Fujian Institute of Research on the Structure of Matter. The large-sized BaF_2 crystal and the LuAG:Ce ceramic samples were produced in the Shanghai Institute of Ceramics, Chinese Academy of Sciences. The BaF_2:Y crystals were produced in the Beijing Glass Research Institute. The YAP:Ce, YAP:Yb, and YAG:Yb crystals were produced in Chengdu Dongjun Laser Co., Ltd. The $LaBr_3$ crystal was produced in Saint-Gobain Crystals.

Photoluminescence (PL) was measured by an Edinburgh Instrument FLS920 fluorescence spectrometer. The signals were detected by a Hamamatsu R928P PMT through a monochromator. Measured PL spectrum was corrected using a calibrated light source. Longitudinal transmittance (LT) was

measured using a Perkin Elmer Lambda-950 spectrometer equipped with double-beam, double-monochromator, and a general purpose optical bench. The systematic uncertainty of the LT measurement is about 0.2%.

Scintillation pulse shape and decay time were measured by a Hamamatsu R2059 PMT and an Agilent 9254 digital scope with a temporal response time of 1.3 and 0.14 ns, respectively, which limited our ability to measure subnanoseconds decay time. In order to measure subnanoseconds of decay time, a Photek MCP-PMT240 and a Tektronix MSO 72304DX were also used for BaF_2 and BaF_2:Y samples, where the corresponding temporal response time is reduced to 0.2 and 0.02 ns, respectively.

LO was measured using either a ^{22}Na or a ^{137}Cs γ-ray source, where the ^{22}Na source provided a coincidence trigger, which helps to mitigate residual phosphorescence in the samples [6], [7]. A Hamamatsu R2059 or a Hamamatsu R1306 PMT was used in the LO measurements, where the PMT R1306 provides a lower gain than the R2059 so was used for samples with a high LO.

The LO of the $LaBr_3$ crystal and LuAG:Ce ceramic samples were measured by the R1306 PMT using 0.662-MeV γ-rays from the ^{137}Cs source. The LO of BaF_2 and BaF_2:Y crystals was measured by the R2059 PMT using 0.511-MeV γ-rays from a ^{22}Na source with a coincidence trigger. The LO of YAP:Ce crystals was measured by the R1306 PMT using 0.511-MeV γ-rays from the ^{22}Na source with a coincidence trigger.

LO was also measured by the R2059 PMT using 5.486-MeV α-rays from an ^{241}Am source for two kinds of samples with a low LO. They are Yb-doped samples suffering with serious thermal quenching, and ZnO:Ga crystals suffering with serious self-absorption. It is well known that the nominal LO values measured by γ-rays and α-rays are different in terms of p.e./MeV, so are not directly comparable. No attempt was made to compare the LO values measured using γ-rays and α-rays. The readers are advised to pay an attention to this difference when reading the LO values listed in Table I.

In all these LO measurements, the samples were wrapped with two layers of Tyvek paper, and the PMTs were coupled to the samples via a thin layer of Down-Corning 200 optical fluid. The systematic uncertainty of the LO measurement is about 1%.

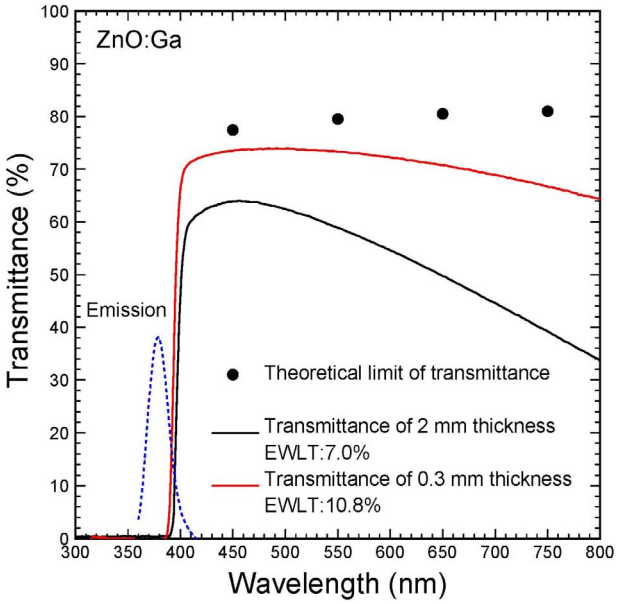

Fig. 3. Transmittance spectra for the ZnO:Ga crystal samples of 33 × 30 × 2 mm^3 and 22 × 22 × 0.3 mm^3.

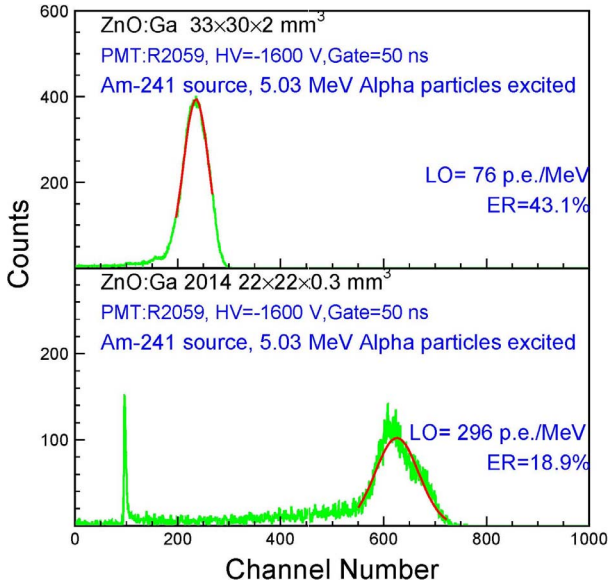

Fig. 4. Pulse height spectra for the ZnO:Ga crystal samples of 33 × 30 × 2 mm^3 and 22 × 22 × 0.3 mm^3 excited by 5.03-MeV α-rays.

III. Experimental Results

A. ZnO:Ga Plates

Gallium-doped ZnO crystal was developed as a Wannier exciton-based scintillator with subnanoseconds of decay time [8], [9], and is commercially available [10]. In such direct-gap semiconductors, the electrons in the conduction band recombine directly with holes in the valence band resulting in near band-edge luminescence [9]. Because of the small Stokes shift, most of the generated emission light in such scintillators is self-absorbed at room temperature.

Fig. 3 shows the transmittance spectra for two ZnO:Ga crystal samples of 2- and 0.3-mm thickness. Also shown in the figure is the photoluminescence spectrum (blue dashed line). Since the scintillation emission of ZnO:Ga peaks at 380 nm which is shorter than its intrinsic cutoff edge of 400 nm, a large fraction of the emission spectrum is self-absorbed in the crystal bulk.

Fig. 4 shows very different peak values of 5-MeV α-rays for these two samples with different thickness. The 5-MeV α-rays excited only a thin-layer crystal at the crystal's surface because of their very short absorption length in the crystal. Since most scintillation photons generated by the α-rays propagated across the entire thickness before reaching the photodetector, the pulse height of the 5-MeV α-rays is thus sample thickness dependent. Consequently, the 0.3-mm thick sample provides a much higher LO for 5-MeV α-rays than the 2-mm-thick sample.

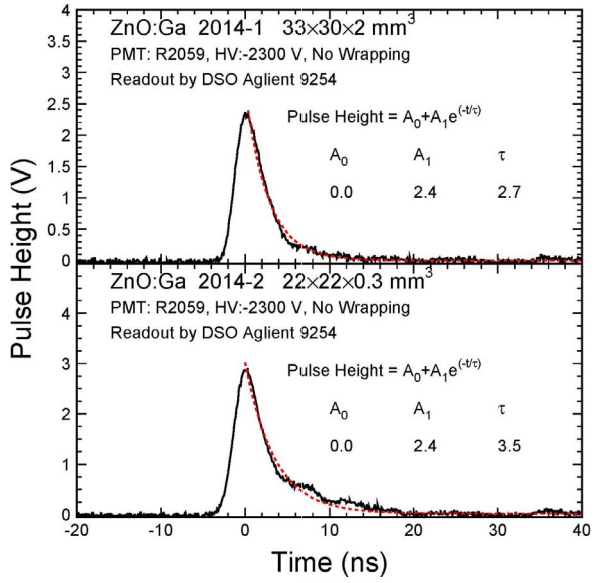

Fig. 5. Pulse shape for the ZnO:Ga samples of 33 × 30 × 2 mm^3 and 22 × 22 × 0.3 mm^3 excited by ^{22}Na γ-rays.

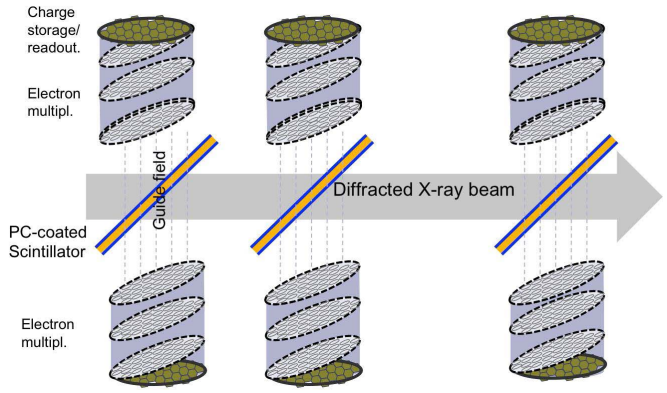

Fig. 6. Schematic showing the multilayer detector architecture for efficient and fast imaging of diffracted X-rays [11].

Fig. 5 shows the pulse shape of two ZnO:Ga samples excited by 0.511-MeV γ-ray from a ^{22}Na source. The observed decay time is a few nanoseconds, which is longer than the 0.5-ns decay time observed from the ZnO:Ga nanoparticles embedded in polystyrene [5]. This difference is partly due to the temporal response time of the R2059 PMT used in this measurement.

The self-absorption restricts applications of ZnO:Ga crystal in bulk for a total absorption front imager. An alternative approach is to develop ZnO:Ga nanoparticle-based front imager for gigahertz hard X-ray imaging [11]. Fig. 6 shows this imager concept for gigahertz X-ray imaging featured with a multilayer high QE photocathode coated with ZnO:Ga nanoparticles. Recently discovered enhanced UV emission in Ag/Au ZnO core–shell nanoparticles hints an interesting approach to develop such thin film-based concept [12].

B. BaF_2 and BaF_2:Y Crystals

In the core valence transition scintillators, such as BaF_2 and CsF, the energy gap between the valence band and the uppermost core band is less than the fundamental bandgap [13], [14]. A photon is emitted when an electron in the valence band fills an ionization hole in the top core band. This is an allowed process with a decay time of an order of 1 ns or less [15]. The overall light yield of core valence scintillation is low due to the inefficiency of creating holes in an upper core band. Because of its fast decay time, however, the light yield in the first nanoseconds is comparable to bright scintillators, such as LYSO:Ce. Such a scintillator has attracted the HEP community pursuing ultrafast calorimeter and/or ultrafast timing.

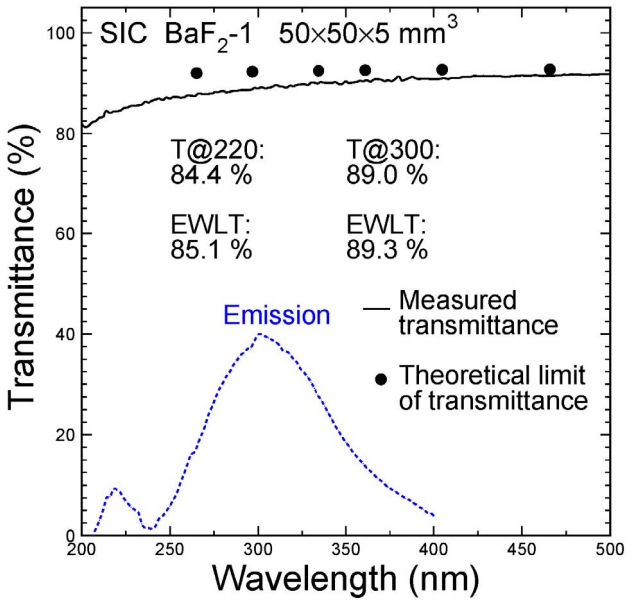

Fig. 7. Transmittance spectrum for the BaF_2 sample of 50 × 50 × 5 mm^3.

Fig. 7 shows transmittance spectrum for the 5-mm-thick BaF_2 crystal sample. Also shown in this plot is the numerical values of the emission weighted longitudinal transmittance (EWLT) for the fast (220 nm with subnanoseconds of decay time) and slow (300 nm with 600-ns decay time) components. We note that BaF_2 has a good transmittance without self-absorption, and the slow component has an intensity of a factor of five of the fast component measured by a PMT with a bialkali photocathode. The slow scintillation component would cause pileup, so needs to be suppressed for these applications.

Fig. 8 shows the pulse height spectrum with a full-width at half-maximum (FWHM) resolution of 54.9% for 0.511-MeV γ-rays from a ^{22}Na source for the BaF_2 sample. The LO is 209 p.e./MeV measured with an integration time of 50 ns.

Fig. 9 compares the pulse shape for BaF_2 samples measured by a Hamamatsu PMT R2059 (top) and a Photek MCP-PMT240 (bottom), respectively. While R2059 data show both rising and decay times of 1.4 ns, which is limited by PMT's temporal response time, they are 0.26 and 0.52 ns, respectively, measured by an MCP-PMT240, indicating that the intrinsic rising time is very small, and its fast scintillation decay time is less than 0.6 ns. We also note that BaF_2 is the only crystal scintillator that can provide subnanoseconds pulsewidth, so is the best choice when ultrafast timing is required.

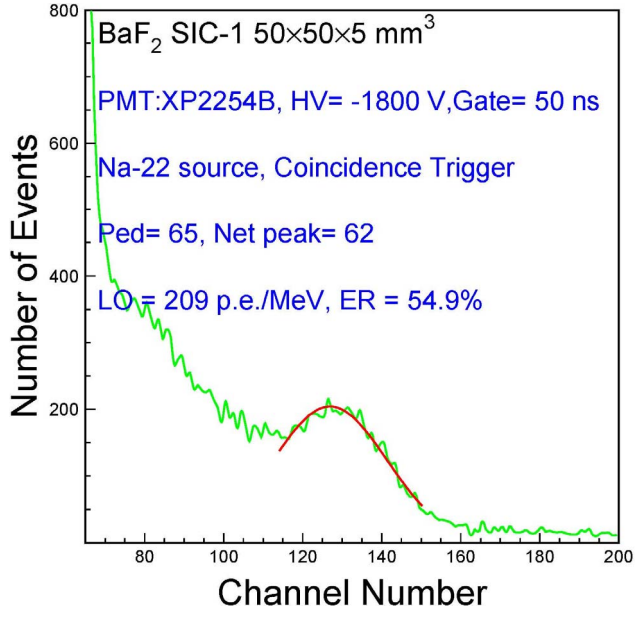

Fig. 8. Pulse height spectrum for the BaF_2 sample of 50 × 50 × 5 mm^3.

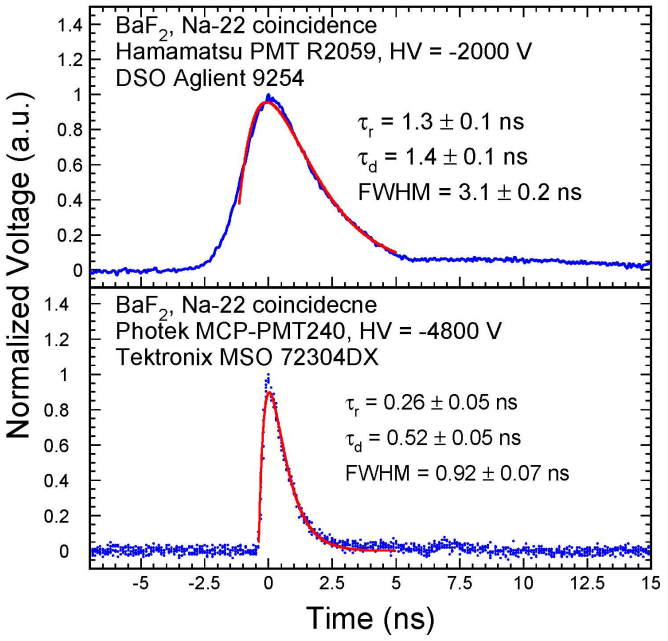

Fig. 9. Normalized pulse shape for a BaF_2 sample excited by ^{22}Na γ-rays, measured by a Hamamatsu R2059 PMT (top) and a Photek MCP-PMT240 (bottom), respectively.

Fig. 10 compares the LO as a function of integration time measured by a Hamamatsu R2059 PMT for an undoped BaF_2 and a yttrium-doped BaF_2:Y samples of the same dimension. Simple exponential fits were used to extract amplitudes for a fast scintillation component and a slow component and its decay time. It is interesting to note that yttrium doping greatly suppressed the slow component. Yttrium-doped BaF_2:Y has thus a great potential to be developed to an ultrafast scintillator in bulk. While the initial result of the BaF_2:Y crystal was reported elsewhere [16], it is our plan to further investigate this material for its use in total absorption front imager shown in Fig. 1 for gigahertz hard X-ray imaging.

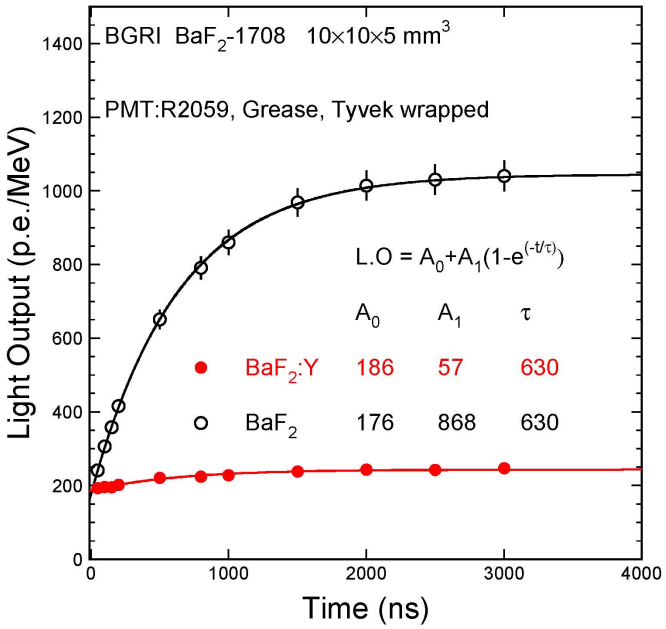

Fig. 10. LO and decay kinetics for BaF_2 and BaF_2:Y samples.

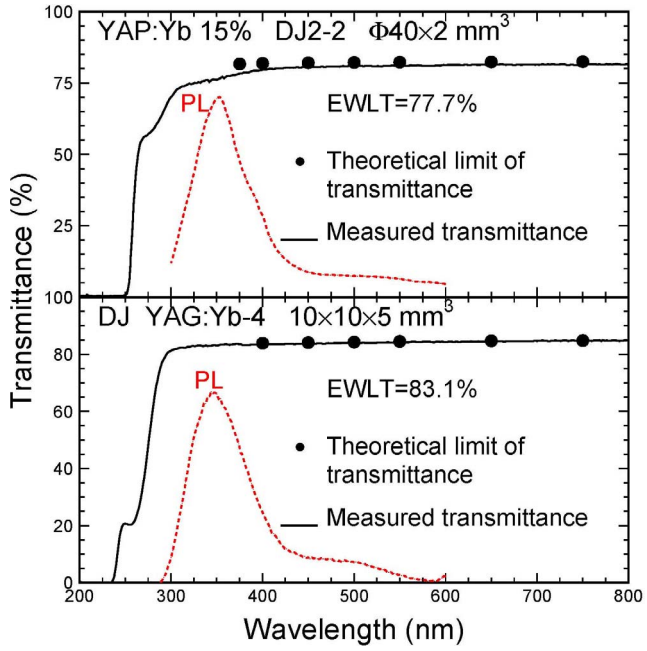

Fig. 11. Transmittance spectra for the YAP:Yb sample (top) of Φ40 × 2 mm^3 and the YAG:Yb sample (bottom) of 10 × 10 × 5 mm^3.

C. Yb^{3+} Activated Scintillators

Yb-doped yttrium perovskites ($YAlO_3$, YAP) [17] and aluminum garnets ($Y_3Al_5O_{12}$, YAG) [18] were commercially developed as IR laser media. Yb^{3+} ions embedded into various host lattices show charge transfer (CT) luminescence [19], [20]. CT luminescence has two bands UV (CT state $\rightarrow^2 F_{7/2}$) and visible (CT state $\rightarrow^2 F_{5/2}$), and exhibits with a strong thermal quenching. Scintillation performances of YAP:Yb and YAG:Yb are very similar and very fast, from a few to tens of nanoseconds depending on

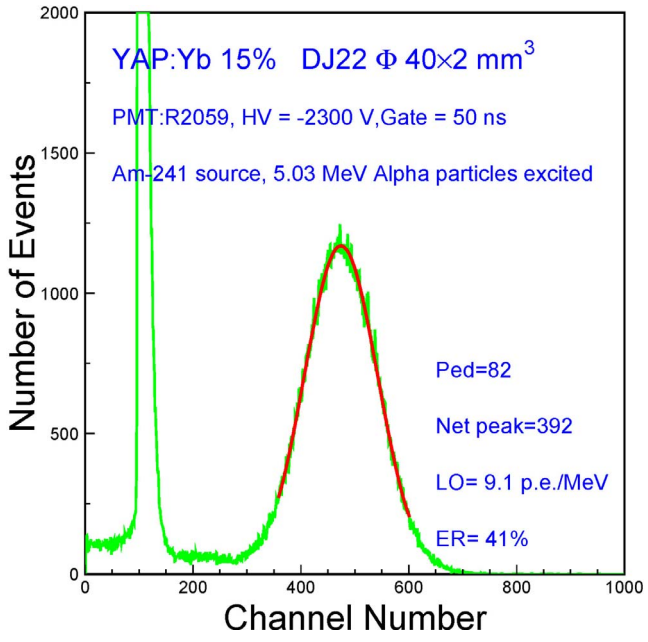

Fig. 12. Pulse height spectrum for the YAP:Yb sample of Φ40× 2 mm^3.

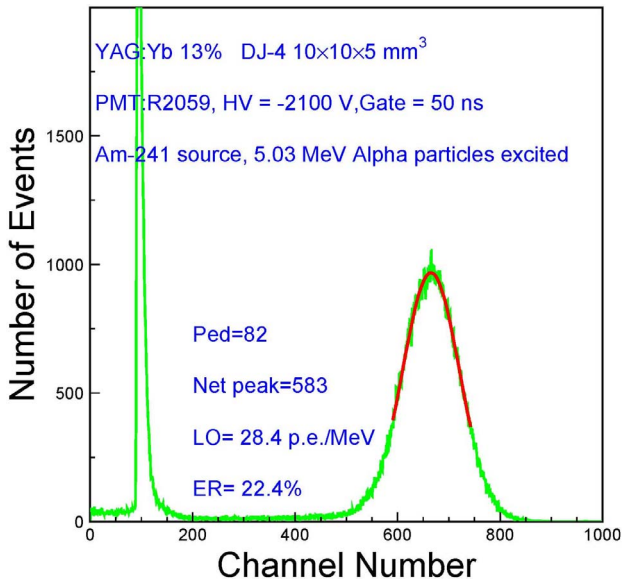

Fig. 13. Pulse height spectrum for the YAG:Yb sample of 10 × 10 × 5 mm^3.

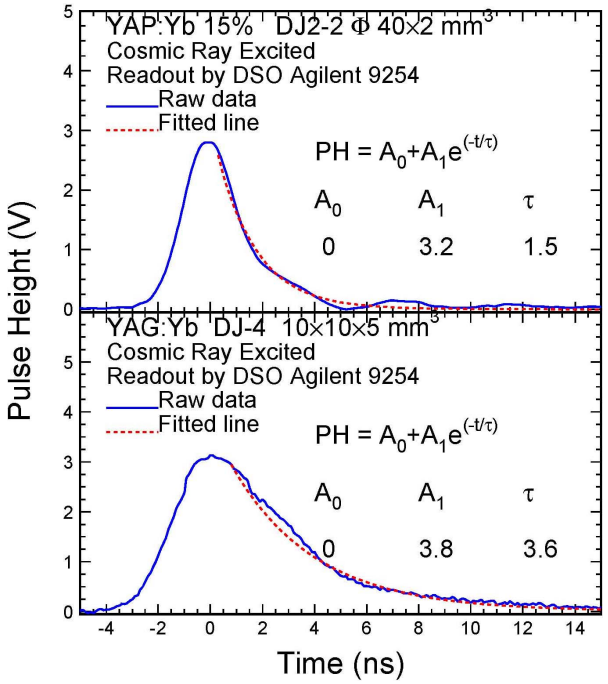

Fig. 14. Pulse shape for the YAP:Yb sample of Φ40× 2 mm^3 and the YAG:Yb sample of 10 × 10 × 5 mm^3 excited by cosmic rays.

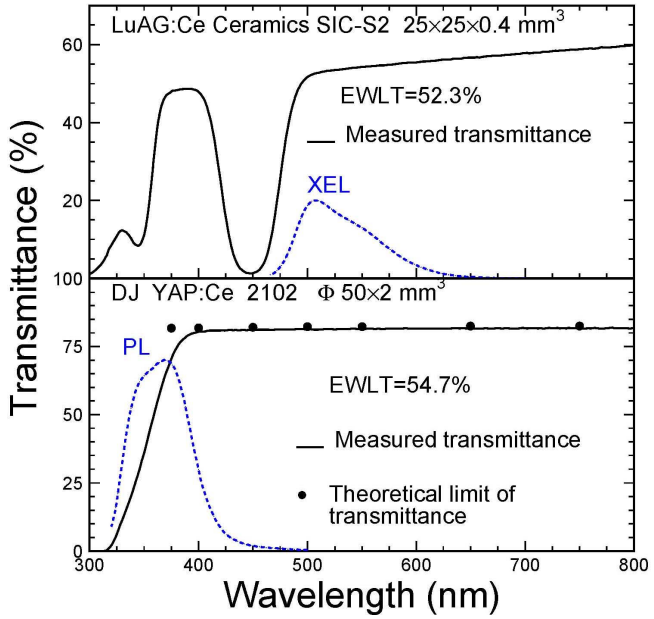

Fig. 15. Transmittance spectra for the LuAG:Ce ceramic sample (top) of 25 × 25 × 0.4 mm^3 and the YAP:Ce sample (bottom) of Φ50 × 2 mm^3.

the temperature, the nature of excitation, and the sample composition [21].

Fig. 11 shows transmittance spectra for the YAP:Yb (top) and YAG:Yb (bottom) crystals. The emission peak for YAP:Yb and YAG:Yb crystals is well within the transparent region of the transmittance spectra, indicating no self-absorption.

Figs. 12 and 13 show the pulse height spectra for two crystals excited by 5.03-MeV α-rays from an ^{241}Am source. The LO of YAP:Yb and YAG:Yb are 9.1 and 28.4 p.e./MeV with the FWHM energy resolution of 41% and 22.4%, respectively. This low LO is due to thermal quenching.

Fig. 14 shows the pulse shape for both crystals excited by cosmic rays. The decay times of 1.5 and 3.6 ns, where 1.5 ns is certainly limited by the temporal response time of the R2059 PMT used in the measurements. In a brief summary, YAP:Yb might be used in low-temperature applications, where a compromise between the LO and the decay time will have to be considered.

D. Ce^{3+}-Activated Scintillators

Ce^{3+}-activated scintillators, such as $LaBr_3$:Ce, LuAG:Ce, and YAP:Ce, show a high LO and a good energy resolution,

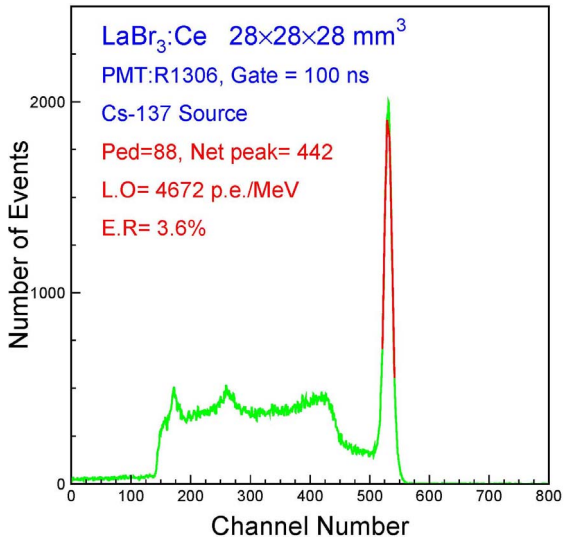

Fig. 16. Pulse height spectrum for the $LaBr_3$:Ce sample of $28 \times 28 \times 28$ mm^3.

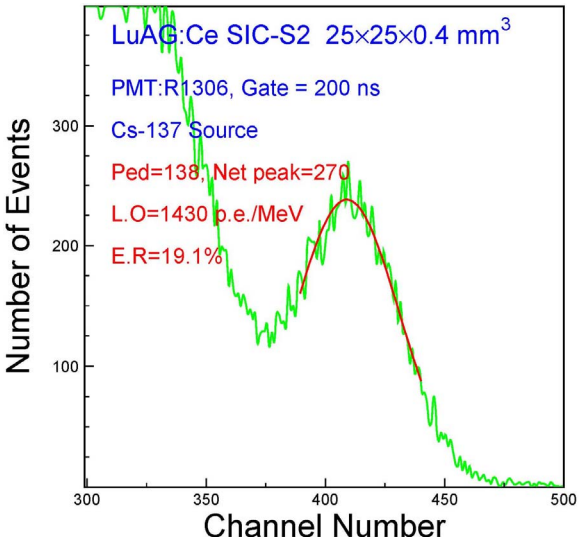

Fig. 17. Pulse height spectrum for the LuAG:Ce ceramic sample of $25 \times 25 \times 0.4$ mm^3.

and a moderate decay time for the parity-allowed Ce^{3+} 5d–4f transition. The fundamental limit of the decay time for Ce^{3+}-activated inorganic compounds, however, is around 15–17 ns [22], which appears too long for gigahertz hard X-ray imaging where the interframe time is of a few nanoseconds.

Fig. 15 shows the transmittance spectra for the LuAG:Ce ceramic sample (top) and the YAP:Ce crystal sample (bottom). The transmittance of LuAG:Ce is much poorer than the theoretical limit because of the scattering centers in this ceramic sample. Also, shown in the figure are the emission spectra for LuAG:Ce and YAP:Ce excited by X-ray and photons, respectively. While the 500-nm emission peak for LuAG:Ce is well within the transmittance region, self-absorption is observed in the YAP:Ce sample.

Figs. 16–18 show pulse height spectrum for the $LaBr_3$:Ce crystal, the LuAG:Ce ceramic, and the YAP:Ce crystal samples, respectively. The $LaBr_3$:Ce sample shows an

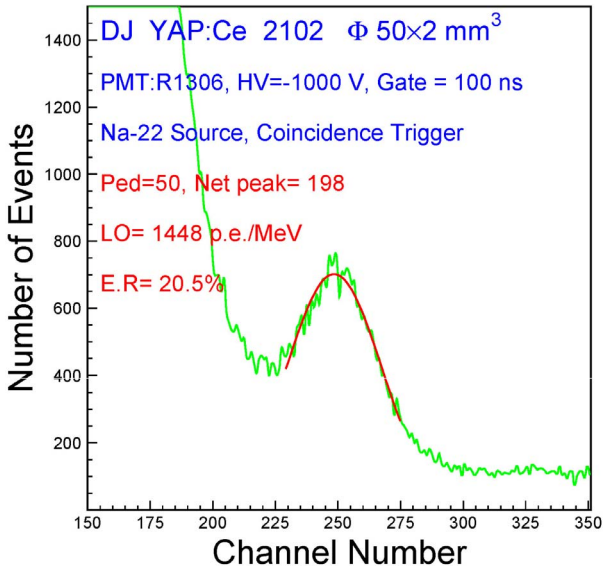

Fig. 18. Pulse height spectrum for the YAP:Ce crystal sample of $\Phi 50 \times 2$ mm^3.

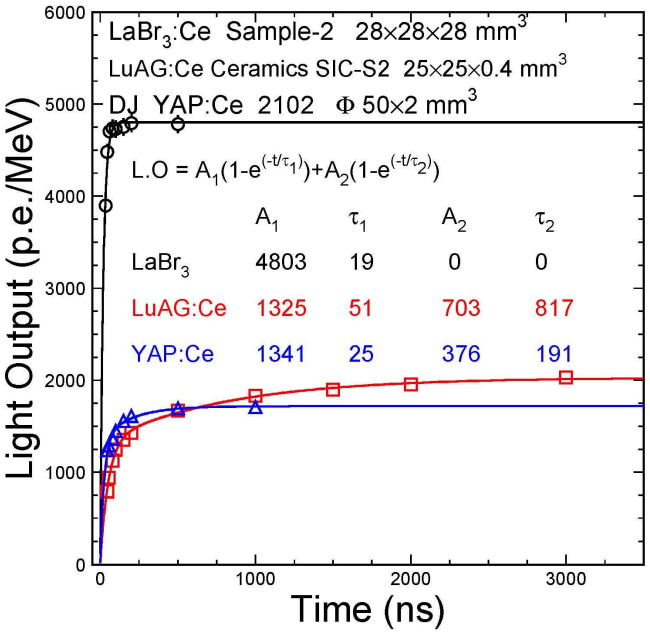

Fig. 19. LO and decay kinetics for the $LaBr_3$ crystal sample (circles), the LuAG:Ce ceramics sample (squares), and the YAP:Ce crystal sample (triangles).

excellent FWHM energy resolution of 3.6%, and a high LO of 4670 p.e./MeV. The LuAG:Ce ceramic sample and the YAP:Ce sample also show good FWHM energy resolutions of 19.1% and 20.5% with LO values of 1430 and 1450 p.e./MeV, respectively.

Fig. 19 compares the LO as a function of integration time for $LaBr_3$ crystal (black circle), LuAG:Ce ceramic (red cubic), and YAP:Ce crystal (blue triangle). $LaBr_3$ crystal shows the highest LO and shortest decay time of 18 ns, which reaches the fundamental limit for Ce^{3+} activated scintillators [22]. Both LuAG:Ce and YAP:Ce show slow component caused by the delay recombination of electrons freed from the electron traps.

IV. Conclusion

A comparative study on four groups of scintillators was carried out for gigahertz hard X-ray imaging. The direct-gap semiconductor ZnO:Ga crystals show a very short decay time, but a low LO because of self-absorption. An imager consisting of ZnO:Ga nanoparticles-based multilayers is one detector concept to be pursued for gigahertz hard X-ray imaging for the proposed MaRIE project.

BaF_2 provides a fast scintillation component with an ultrafast decay time of less than 0.6 ns and an ultrashort FWHM pulsewidth of less than nanoseconds, providing a solid foundation for an ultrafast scintillator. Its slow scintillation component with 600-ns decay time may be suppressed effectively by Y^{3+} doping. An imager consisting of bulk BaF_2:Y crystals may serve as a total absorption detector concept for gigahertz hard X-ray imaging for the proposed MaRIE project.

The Yb^{3+}-doped crystals show very short decay time, but they have low LO due to thermal quenching. The Ce^{3+}-doped scintillators show very high light yield and good FWHM energy resolution. Their decay time, however, is too long for gigahertz hard X-ray imaging.

References

[1] R. W. Garnett and M. S. Gulley, "Matter-radiation interactions in extremes," in *Proc. Linear Accelerator Conf. (LINA)*, 2010, pp. 485–487.

[2] Z. Wang *et al.*, "Gigahertz (GHz) hard X-ray imaging using fast scintillators," *Proc. SPIE, Hard X-Ray, Gamma-Ray, Neutron Detector Phys. XV*, vol. 8852, p. 88521A, Sep. 2013.

[3] P. Denes, S. Gruner, M. Stevens, and Z. Wang, "Ultrafast and high-energy X-ray imaging technologies and applications," Los Alamos Nat. Lab., Santa Fe, NM, USA, Tech. Rep. LA-UR-17-22085, Aug. 2016. [Online]. Available: http://www.lanl.gov/science-innovation/science-facilities/marie/_assets/docs/workshops/ultrafast-high-energy-x-ray.pdf

[4] S. Liu *et al.*, "Towards bright and fast $Lu_3Al_5O_{12}$:Ce,Mg optical ceramics scintillators," *Adv. Opt. Mater.*, vol. 4, no. 5, pp. 731–739, 2016.

[5] P. Lecoq, "The 10 ps timing-of-flight PET challenge," in *Proc. SCINT Conf.*, Chamonix, France, 2017.

[6] R. Y. Zhu *et al.*, "A study on the properties of lead tungstate crystals," *Nucl. Instrum. Methods Phys. Res. A, Accel. Spectrom. Detect. Assoc. Equip.*, vol. 376, no. 3, pp. 319–334, 1996.

[7] J. Chen, R. Mao, L. Zhang, and R. Y. Zhu, "Large size LSO and LYSO crystals for future high energy physics experiments," *IEEE Trans. Nucl. Sci.*, vol. 54, no. 3, pp. 718–724, Jun. 2007.

[8] W. Lehmann, "Edge emission of *n*-type conducting Zno and CdS," *Solid-State Electron.*, vol. 9, nos. 11–12, pp. 1107–1110, 1966.

[9] S. E. Derenzo, M. J. Weber, and M. K. Klintenberg, "Temperature dependence of the fast, near-band-edge scintillation from CuI, HgI_2, PbI_2, ZnO:Ga and CdS:In," *Nucl. Instrum. Methods Phys. Res. A, Accel. Spectrom. Detect. Assoc. Equip.*, vol. 486, pp. 214–219, Jun. 2002.

[10] E. Ohshima *et al.*, "Growth of the 2-in-size bulk ZnO single crystals by the hydrothermal method," *J. Crystal Growth*, vol. 260, nos. 1–2, pp. 166–170, 2004.

[11] Z. Wang *et al.*, "Thin scintillators for ultrafast hard X-ray imaging," *Proc. SPIE, Photon Counting Appl.*, vol. 9504, p. 95040N, May 2015.

[12] E. J. Guidelli, O. Baffa, and D. R. Clarke, "Enhanced UV emission from silver/ZnO and gold/ZnO core-shell nanoparticles: Photoluminescence, radioluminescence, and optically stimulated luminescence," *Sci. Rep.*, vol. 5, Sep. 2015, Art. no. 14004.

[13] A. P. Shpak, O. A. Glike, A. G. Dmitriev, P. A. Rodnyi, A. S. Voloshinovskii, and S. M. Pidzyrailo, "Radiative core-valence transitions in wide-gap crystals," *J. Electron. Spectrosc. Related Phenomena*, vol. 68, pp. 335–338, May 1994.

[14] P. A. Rodnyi, "Core-valence transitions in wide-gap ionic-crystals," *Soviet Phys. Solid-State*, vol. 34, no. 7, pp. 1053–1066, 1992.

[15] M. J. Weber, "Scintillation: mechanisms and new crystals," *Nucl. Instrum. Methods Phys. Res. A, Accel. Spectrom. Detect. Assoc. Equip.*, vol. 527, nos. 1–2, pp. 9–14, 2004.

[16] R.-Y. Zhu, "Applications of very fast inorganic crystal scintillators in future HEP experiments," in *Proc. Technol. Instrum. Particle Phys.*, Beijing, China, May 2017. [Online]. Available: http://www.hep.caltech.edu/~zhu/talks/ryz_170522_Fast_Crystals.pdf

[17] V. E. Kisel, S. V. Kurilchik, A. S. Yasukevich, S. V. Grigoriev, S. A. Smirnova, and N. V. Kuleshov, "Spectroscopy and femtosecond laser performance of Yb^{3+}:$YAlO_3$ crystal," *Opt Lett.*, vol. 33, no. 19, pp. 2194–2196, 2008.

[18] A. R. Reinberg, L. A. Riseberg, R. M. Brown, R. W. Wacker, and W. C. Holton, "GaAs: Si LED pumped Yb-doped YAG laser," *Appl. Phys. Lett.*, vol. 19, no. 1, p. 11, 1971.

[19] L. van Pieterson, M. Heeroma, E. de Heer, and A. Meijerink, "Charge transfer luminescence of Yb^{3+}," *J. Lumin.*, vol. 91, nos. 3–4, pp. 177–193, 2000.

[20] R. Chipaux *et al.*, "Ytterbium-based scintillators, a new class of inorganic scintillators for solar neutrino spectroscopy," *Nucl. Instrum. Methods Phys. Res. A, Accel. Spectrom. Detect. Assoc. Equip.*, vol. 486, pp. 228–233, Jun. 2002.

[21] S. Belogurov, G. Bressi, G. Carugno, and Y. Grishkin, "Properties of Yb-doped scintillators: YAG, YAP, LuAG," *Nucl. Instrum. Methods Phys. Res. A, Accel. Spectrom. Detect. Assoc. Equip.*, vol. 516, no. 1, pp. 58–67, 2004.

[22] P. Dorenbos, "Fundamental limitations in the performance of Ce^{3+}}−, Pr^{3+}−, Eu^{2+}−activated scintillators," *IEEE Trans. Nucl. Sci.*, vol. 57, no. 3, pp. 1162–1167, Jun. 2010.